DRAFT VERSION JUNE 28, 2013
Preprint typeset using LATEX style emulateapj v. 11/10/09

SHORTCOMINGS OF THE SINGLE SERSIC GALAXY PROFILE WHEN ESTIMATING CHROMATIC WEAK LENSING BIASES WITH A RING TEST

J. MEYERS[1]

Draft version June 28, 2013

ABSTRACT

This is the abstract. Lorem ipsum dolor sit amet, consectetuer adipiscing elit. Donec hendrerit tempor tellus. Donec pretium posuere tellus. Proin quam nisl, tincidunt et, mattis eget, convallis nec, purus. Cum sociis natoque penatibus et magnis dis parturient montes, nascetur ridiculus mus. Nulla posuere. Donec vitae dolor. Nullam tristique diam non turpis. Cras placerat accumsan nulla. Nullam rutrum. Nam vestibulum accumsan nisl.

1. INTRODUCTION

Cosmic shear experiments aim to constrain cosmological parameters by measuring the small departure from statistical isotropy of distant galaxy shapes induced by the gravitational lensing from foreground large scale structure. The shapes of galaxy images collected from telescopes, however, are not only affected by cosmic shear (typically a $\sim 1\%$ effect), but also by the combined point spread function (PSF) of the atmosphere (for ground-based experiments), telescope optics, and the image sensor (often a few % effect). The shape of this additional convolution kernel is typically constrained from the shapes of stars, which are effectively point sources before being smeared by the PSF. Galaxy images can then be deconvolved with the estimated convolution kernel. Implicit in this approach is the assumption that the galactic kernel is the same as the stellar kernel. Effects that make the PSF dependent on wavelength will violate this assumption, as stars and galaxies at different redshifts, have different spectral energy distributions, and hence different PSFs.

Examples of wavelength-dependent PSF contributions include:

- atmospheric differential chromatic refraction (DCR)
- atmospheric seeing
- telescope optics DCR
- photoconversion depth in the sensor and subsequent charge diffusion

This note will focus on PSF mis-estimations due to the first of the above effects, though the conclusions are applicable to any situation in which the bias due to using the wrong PSF is estimated using a ring test with a simple model parameterization.

2. ANALYTIC EXPECTATIONS

? derived analytic expressions for the bias expected in weak lensing measurements due to differential chromatic refraction. I will summarize the main points of their argument here.

Let $R(\lambda, z_a)$ be the refraction towards the zenith of a photon with wavelength λ and true zenith angle (before refraction) z_A. The refraction can be factored into

$$R(\lambda; z_a) = g(\lambda)\tan(z_a) \tag{1}$$

jmeyers3@stanford.edu
[1] Department of Physics, Stanford University, Stanford, CA 94305

and $g(\lambda)$, which implicitly depends on air pressure, temperature, and the partial pressure of water vapor, and can be obtained from **?** and **?**. On the focal plane, and forr monochromatic sources, the only effect is to move the apparent position of the object. For sources which are not monochromatic (i.e. all real sources), having a wavelength density of surviving photons (i.e. the product of the source photon density and the total system throughput function) given by $\mathrm{p}_\lambda(\lambda)$, the mismatched displacements of different wavelengths introduces a convolution kernel in the zenith direction that can be written in terms of the inverse of Equation 1:

$$h(R) = \frac{p_\lambda(\lambda(R; z_a)) \left|\frac{\mathrm{d}\lambda}{\mathrm{d}R}\right|}{\int p_\lambda(\lambda)\,\mathrm{d}\lambda} \tag{2}$$

This kernel can largely be characterized in terms of its first and second central moments given by:

$$\bar{R} = \int h(R) R\,\mathrm{d}R = \frac{\int R(\lambda; z_a) p_\lambda(\lambda)\,\mathrm{d}\lambda}{\int p_\lambda(\lambda)\,\mathrm{d}\lambda} \tag{3}$$

$$V = \int h(R)(R - \bar{R})^2\,\mathrm{d}R = \frac{\int (R(\lambda; z_a) - \bar{R})^2 p_\lambda(\lambda)\,\mathrm{d}\lambda}{\int p_\lambda(\lambda)\,\mathrm{d}\lambda} \tag{4}$$

Galaxy shapes can be characterized by the quadrupole moments of their light distribution given by:

$$I_{\mu\nu} = \frac{1}{f}\int \mathrm{d}x\,\mathrm{d}y I(x,y)\mu - \bar{\mu}(\nu - \bar{\nu}) \tag{5}$$

$$\bar{\mu} = \frac{1}{f}\int \mathrm{d}x\,\mathrm{d}y I(x,y)\mu \tag{6}$$

$$f = \int \mathrm{d}x\,\mathrm{d}y I(x,y) \tag{7}$$

In particular, galaxy size and 2-component ellipticity are frequently defined as:

$$r^2 = I_{xx} + I_{yy} \tag{8}$$

$$e_1 = \frac{I_{xx} - I_{yy}}{r^2} \tag{9}$$

$$e_2 = \frac{2I_{xy}}{r^2} \tag{10}$$

For the case of differential chromatic refraction, we can set, without loss of generality, the x direction to be towards zenith.

The effect of DCR is then to take $I_{xx} \to I_{xx} + V$, which also takes $r^2 \to r^2 + V$, but leaves I_{yy} and I_{xy} unchanged. The ellipticity and size parameterizations are defined in terms of the quadrupole moments before the galaxy light distribution is smeared by the PSF, but we only have access to the light distribution after convolution. The second moments before (I^g) and after (I^o) convolution are related via the second moments of the PSF (I^*) like $I^g = I^o - I^*$. If the SED's of galaxies and stars were the same, then the effect of DCR would be to add V to both I^o and I^*, which would then cancel when computing I^g and subsequently galaxy shape parameters. The differences between stellar and galactic SEDs, however, will introduce a small error $\Delta V \ll r^2$ into I_{xx} and r^2, which leads to biases in the derived ellipticity parameters:

$$e_1 \to \frac{I_{xx} + I_{yy} + \Delta V}{r^2 + \Delta V} \approx e_1 \left(1 + \frac{\Delta V}{r^2}\right) + \frac{\Delta V}{r^2} \tag{11}$$

$$e_2 \to \frac{2 I_{xy}}{r^2 + \Delta V} \approx e_2 \left(1 + \frac{\Delta V}{r^2}\right) \tag{12}$$

Under the expectation that $\langle e_i \rangle \approx 2\gamma_i$ and defining the shear calibration parameters m and c such that $\hat{\gamma} = \gamma(1 + m) + c$, where $\hat{\gamma}$ indicates the estimator for the true shear γ, we reach the expectation that $m = \frac{\Delta V}{r^2}$, $c_1 = m/2$, and $c_2 = 0$. Note that nowhere in the above analysis is there any assumption on the profile of the galaxy in question.

3. RING TEST

An alternative way to estimate the bias in $\hat{\gamma}$ induced by DCR is to simulate galaxy images using the "true" (galactic) PSF and then attempt to recover the simulated galactic ellipticities while pretending that the PSF is "wrong" (stellar). A ring test (**?**) is a specific prescription for such a suite of simulations designed to rapidly converge to the correct value of $\hat{\gamma}$. The test gets its name from the arrangement of galaxy shapes used in the simulated images, which form a ring in ellipticity space (i.e. constant $|e|$), before any shear is applied. By choosing intrinsic ellipticities that exactly average to zero, the results of the test converge faster than for randomly (but isotropically) chosen ellipticities that only average to zero statistically.

The general procedure can be implemented as follows:

1. Choose an input "true" reduced shear g
2. Choose a pre-sheared ellipticity $e^s = (e_1^s, e_2^s)$
3. Compute the sheared ellipticity from $e^o = \frac{e^s + g}{1 + g^* e^s}$
4. Generate a "truth" image by convolving the galaxy model with the "true" PSF (galactic in this case)
5. Using a "reconstruction" PSF (stellar in this case), find the best fitting model to the "truth" image, record the measured ellipticity from the model parameters
6. Repeat steps 3-5 using the opposite pre-sheared ellipticity $-e^s$
7. Repeat steps 2-6 for as many values around the ellipticity ring as desired
8. Average all recorded output ellipticity values. This is the shear estimate $\hat{g}$
9. Repeat steps 1-8 to map out the relation $g(\hat{g})$
10. m and c are the slope and intercept of the best-fit linear relation between g and $\hat{g}$ (note we assume that $g \approx \gamma$)

As described above, the ring test requires some prescription for creating galaxy images with a given ellipticity. Here I investigate using a single Sersic profile as the galaxy model. The Sersic profile has 7 parameters: the x and y coordinates of the center, the total flux, the effective radius r_e (also called the half-light radius), the two component ellipticity $\mathbf{e}$, and the Sersic index n. Using r as an elliptical radial coordinate, the profile shape is:

$$I(r) \propto \mathrm{e}^{[-k(r/r_e)^2]^{\frac{1}{2n}}} \tag{13}$$

The constant $k \approx 1.9992n - 0.3271$ is chosen such that r_e is the half-light radius for a circularized profile. Limiting cases of the Sersic profile include the Gaussian profile which has $n = 0.5$, an exponential profile which has $n = 1.0$, and a de Vaucouleurs profile which has $n = 4.0$. The profile ranges from smoothly peaked with small tails at low n (such as an $n = 0.5$ Gaussian), to very sharply peak with heavy tails (such as an $n = 4.0$ deVaucoulers profile).

In addition to a galaxy model, the ring test also requires a model for the PSF. We have described above the PSF kernel that describes the contribution of DCR, but other contributions to the PSF also exist, due to atmospheric turbulence, telescope optics, and the detector for example. Ground based telescope PSFs are usually dominated by atmospheric turbulence, and are frequently modeled by a Moffat profile:

$$I_p(r) \propto \left(1 + \left(\frac{r}{\alpha}\right)^2\right)^{-\beta} \tag{14}$$

$$\alpha = \frac{\mathrm{FWHM}}{2\sqrt{2^{1/\beta} - 1}} \tag{15}$$

The PSF used in the ring test in this note is based on a Moffat profile with a FWHM of $0\farcs7$ and softening parameter $\beta = 2.6$. This base PSF is then convolved (in the zenith direction only) with the DCR kernel given in Equation 2. The "true" PSF uses a DCR kernel derived from a galaxy SED, while the "reconstruction" PSF uses a DCR kernel derived from a stellar SED.

4. SERSIC INDEX DEPENDENCE

Compare analytic expression with ring test results for different Sersic indices.

5. FAILURE OF RING TEST

Attempt to explain why the ring test fails for high Sersic index galaxies.

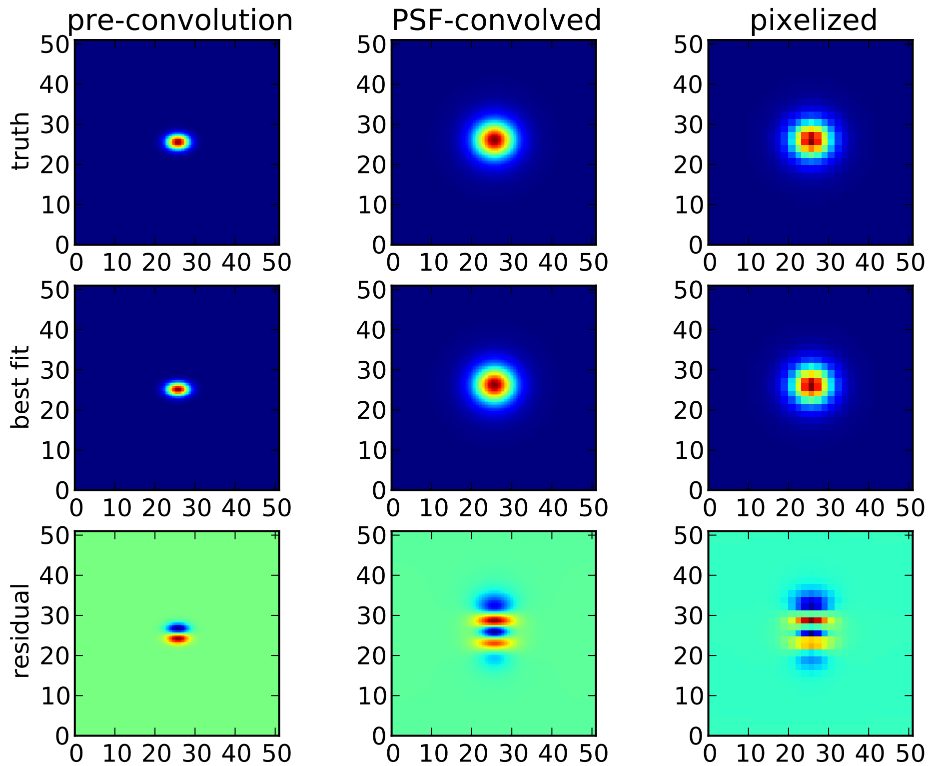

FIG. 1.— Lorem ipsum dolor sit amet, consectetuer adipiscing elit. Praesent libero orci, auctor sed, faucibus vestibulum, gravida vitae, arcu. Nunc posuere. Suspendisse potenti. Praesent in arcu ac nisl ultricies ultricies. Fusce eros. Sed pulvinar vehicula ante. Maecenas urna dolor, egestas vel, tristique et, porta eu, leo. Curabitur vitae sem eget arcu laoreet vulputate. Cras orci neque, faucibus et, rhoncus ac, venenatis ac, magna. Aenean eu lacus. Aliquam luctus facilisis augue. Nullam fringilla consectetuer sapien. Aenean neque augue, bibendum a, feugiat id, lobortis vel, nunc. Suspendisse in nibh quis erat condimentum pretium. Vestibulum tempor odio et leo. Sed sodales vestibulum justo. Cras convallis pellentesque augue. In eu magna. In pede turpis, feugiat pulvinar, sodales eget, bibendum consectetuer, magna. Pellentesque vitae augue.

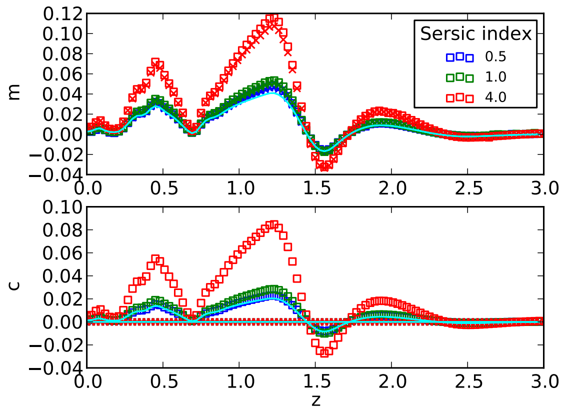

FIG. 2.— Lorem ipsum dolor sit amet, consectetuer adipiscing elit. Praesent libero orci, auctor sed, faucibus vestibulum, gravida vitae, arcu. Nunc posuere. Suspendisse potenti. Praesent in arcu ac nisl ultricies ultricies. Fusce eros. Sed pulvinar vehicula ante. Maecenas urna dolor, egestas vel, tristique et, porta eu, leo. Curabitur vitae sem eget arcu laoreet vulputate. Cras orci neque, faucibus et, rhoncus ac, venenatis ac, magna. Aenean eu lacus. Aliquam luctus facilisis augue. Nullam fringilla consectetuer sapien. Aenean neque augue, bibendum a, feugiat id, lobortis vel, nunc. Suspendisse in nibh quis erat condimentum pretium. Vestibulum tempor odio et leo. Sed sodales vestibulum justo. Cras convallis pellentesque augue. In eu magna. In pede turpis, feugiat pulvinar, sodales eget, bibendum consectetuer, magna. Pellentesque vitae augue.